

Local temperature rise during the electron beam characterization

Calculation model for the $\text{Al}_x\text{Ga}_{1-x}\text{N}$ at low dimensions

LAZHAR LEGHRIB, ABDELKADER NOURI*

LMSSEF Laboratory and LCAM Laboratory, University of Oum El-Bouaghi, 04000, Algeria

During the characterization by electron beam techniques including scanning electron microscope (SEM) and cathodoluminescence at low dimensions, some undesirable phenomena (unwanted effects) can be created, like the thermal effects (or electron beam damage), and these effects can damage the sample. This limits the information one can get from a sample or reduces image spatial resolution. In order to understand these effects, significant efforts have been made but these studies focused on the thermal properties, without a detailed study of the causes of nanoscale heating in the bulk of samples during the SEM-characterization. Additionally, it is very difficult to measure experimentally the heating because there are many variables that can affect the results, such as the current beam, accelerating energy, thermal conductivity and size of samples. Taking into account all the factors and in order to determine the local temperature rise during the electron beam characterization of AlGa_xN at low dimensions, we have used a hybrid model based on combined molecular dynamics and Monte Carlo calculation of inelastic interaction of electrons with matter to calculate the temperature elevation during the SEM-characterization which can be taken into account during the characterization of AlGa_xN at low dimension by electron beam techniques.

Keywords: *semiconductors; aluminum gallium nitride (AlGa_xN); scanning electron microscope (SEM); thermal effects*

1. Introduction

Gallium nitride (GaN) is a good candidate for the realization of optical and optoelectronic components dedicated to telecom applications such as blue ultraviolet (UV) light-emitting diodes (LEDs), and high-temperature/high-power electronic devices, high electron mobility transistors (HEMTs) and lasers diodes (LDs) [1]. GaN nanotubes are proposed for applications in nanoscale electronics, optoelectronics and biochemical sensing applications [2]. The characterization of these semiconductor compounds using electron beam techniques which is based on the electrons-matter interaction offers many benefits [3–5]. Generally, the electron-matter interactions (scattering events) can be divided into two categories; elastic and inelastic interactions [6]. The energy transferred from an incident electron beam (inelastic interaction) to the specimen can cause collective vibrations of atoms

(phonons generation); these vibrations are equivalent to heat flux in the sample. In the earliest work by Talmon et al. [7, 8], concerning the existing models for prediction of temperature increase in samples during electron-beam exposure, they developed a numerical model to estimate the electron-beam heating problem on 2-D thin film specimens. In the recent work by Randolph et al. [9], in order to determine the magnitude of electron-beam-induced heating (EBIH) on a nanofiber tip and a SiO₂ thin film as a function of current beam energy and sample geometry, they employed a Monte Carlo electron-solid interaction model integrated with a finite element. However, at nanoscale Nouri et al. [10] demonstrated that a small change in the primary beam current can greatly increase the degree of surface heating, particularly at lower accelerating voltages.

Finally, in the recently performed work by Nouri [11], he introduced the molecular dynamics with Monte Carlo method to estimate the influence of analysis duration on the thermal effect.

*E-mail: nouiri_kader@yahoo.fr

The calculation of the thermal effect induced by electron beam during the characterization of GaN nanostructures has been studied recently [12]. In the present work, we have studied low-dimensional $\text{Al}_x\text{Ga}_{1-x}\text{N}$ structures (1 μm to 8 μm), in particular for $x = 0.5$ in terms of their applications in photonic devices (blue emission) and the thickness effects of $\text{Al}_{0.5}\text{Ga}_{0.5}\text{N}$ barriers on the optical properties of AlGaN multiquantum wells [13].

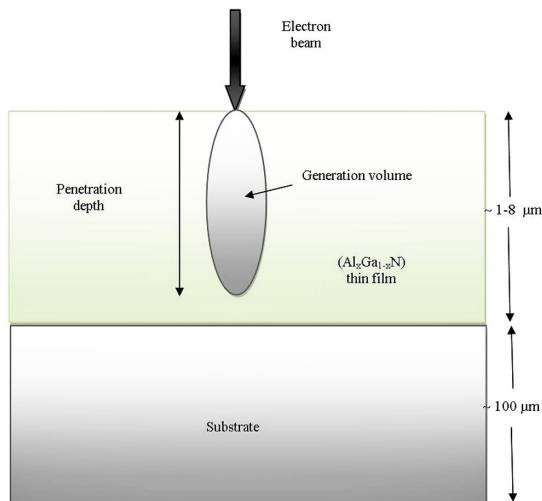


Fig. 1. Schematic representation of electron beam characterization techniques.

2. Calculation procedure

Scattering mechanisms can be divided into elastic and inelastic. The elastic scattering of electrons by the nuclei of the atoms which are partially screened by the bound electrons, can be analyzed using the Rutherford model. The inelastic scattering occurs by several mechanisms inside the material. In this model, we study a semiconductor material (AlGaN), in which there are three principal processes:

- backscattered electrons (elastic scattering);
- generation of electron-hole pairs (inelastic scattering);
- excitation of lattice oscillations (phonons) (inelastic scattering).

The studied material is considered as an $\text{Al}_x\text{Ga}_{1-x}\text{N}$ thin film (1 μm to 8 μm) with different values of aluminum fraction x . The temperature rise is calculated for $x = 0.5$.

When an electron beam is focused on a material, various elastic and inelastic interactions can occur between the electron and the material (Fig. 1). The number of phonons created along the electron trajectory is calculated numerically to observe the variation of temperature rise as a function of depth which will be presented for different acceleration energies, electron beam currents, and for different scanning durations. Calculation of temperature distribution due to the incident electron beam depends on the penetration depth, and for this reason, the sample is divided into several half-spherical zones. In each area, there is an excess of electron-hole (e-h) pairs (Δn) and phonons (Δph). The excess of e-h pairs (Δn) (in case of electron beam induced current, EBIC) will be converted to photocurrent by applying an external electric field [14] or converted into light by radiative recombination (cathodoluminescence) [15]. In our case, we are interested in phonons that appear as a temperature ΔT rise. After each collision, the electron loses an average energy of $E_{moy} = 38.8$ meV.

To determine the temperature rise, it is assumed that after each collision, one (e-h) pair and one phonon are generated in the lattice. The thermal energy dissipated to create a phonon is calculated using the mean thermal energy of atom which is given by:

$$E_{moy} = \frac{3}{2}k_B T \quad (1)$$

where $k_B = 1.38 \times 10^{-23}$ J·K⁻¹, T is temperature [K].

The phonon energy excess (ΔQ_i) per unit volume is calculated as the mean thermal energy E_{moy} times the total number of phonons Δph inside the volume of each zone V_i ; this energy excess is transformed into a temperature rise ΔT_i :

$$\Delta T_i = \frac{\Delta Q_i}{\rho \cdot C_p} \quad (2)$$

where ρ is the density (mass in cubic centimeter) and C_p is the specific heat.

The specific heat C_p of wurtzite GaN at a constant pressure for $298 \text{ K} < T < 1773 \text{ K}$ [16]:

$$C_p = 38.1 + 8.96 \times 10^{-3} T \text{ (J}\cdot\text{mol}^{-1}\cdot\text{K)},$$

$$\rho = 6095 \text{ kg}\cdot\text{m}^{-3} \text{ for GaN.}$$

Taking into account the dissipation of heat outside, caused by thermal conduction, the heat flux from zone $i-1$ to zone i is written [10] as:

$$\Delta H_i = k \cdot a \cdot \left(\frac{T_{i-1} - T_i}{l} \right) \quad (3)$$

Thermal conductivity, k at room temperature is about 25 W/mK for $0.2 < x < 0.8$ and $k = 130 \text{ W/mK}$ to 200 W/mK for GaN [17], a is the surface area of zone i , l is the distance between the middle of zone $i-1$ and the middle of zone i . l is equal to the thickness of zone i because all the zones have the same thickness.

More detailed calculation procedures and explanations are available in Nouiri model [11]. In this study, we have used the $\text{Al}_x\text{Ga}_{1-x}\text{N}$ parameters taking into account the Al contents (x) (AlN mole fraction):

$$a(x) = 3.1986 - 0.0891x \text{ (\AA)},$$

$$c(x) = 5.2262 - 0.2323x \text{ (\AA)},$$

$$E_g(x) = xE_g(\text{AlN}) + (1-x)E_g(\text{GaN}) - bx(1-x),$$

where $E_g(\text{AlN}) = 6.1 \text{ eV}$, $E_g(\text{GaN}) = 3.4 \text{ eV}$ and b is the bowing parameter.

3. Results and discussion

3.1. Penetration depth

Our calculation for GaN [12] is generally similar to other models [18–20] and it is comparable with that obtained by As et al. [21]. Fig. 2 presents the maximum penetration depth of electrons calculated for $\text{Al}_x\text{Ga}_{1-x}\text{N}$ for different values of content x as a function of accelerating voltage. The penetration depth decreases when the aluminum fraction increases.

3.2. Temperature rise

Fig. 3 shows the temperature rise in AlN, GaN and $\text{Al}_{0.5}\text{Ga}_{0.5}\text{N}$ respectively, as a function of depth when the accelerating energy is equal to 8 keV ,

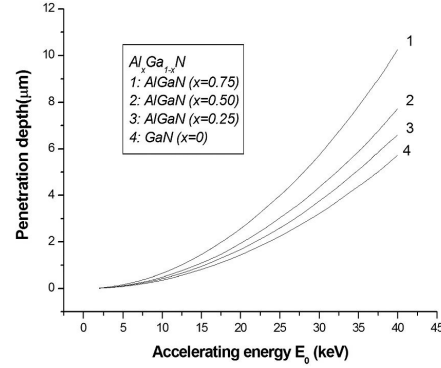


Fig. 2. Penetration depth of electrons in $\text{Al}_x\text{Ga}_{1-x}\text{N}$ with different values of content x as a function of accelerating energy.

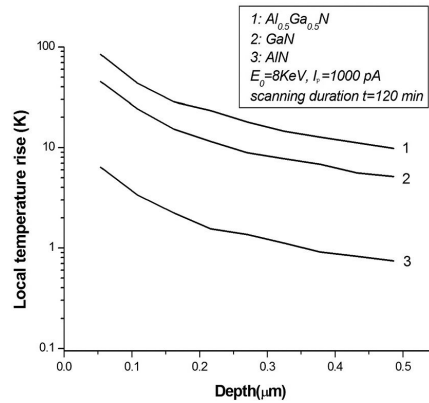


Fig. 3. Temperature rise as a function of depth in AlN, GaN and $\text{Al}_{0.5}\text{Ga}_{0.5}\text{N}$

current beam is $I_p = 1000 \text{ pA}$ and the scanning duration is 120 minutes. It appears clearly that the magnitude of local temperature rise in case of $\text{Al}_{0.5}\text{Ga}_{0.5}\text{N}$ is greater than that of GaN and AlN respectively. This may be explained by the thermal conductivities of each compound (50 W/mK for $\text{Al}_{0.5}\text{Ga}_{0.5}\text{N}$, 150 W/mK for GaN and 250 W/mK for AlN) [17]. In all cases, the temperature rise takes the highest values at the surface and it decreases exponentially with depth.

3.3. Influence of the accelerating energy (voltage)

Fig. 4 shows the local temperature rise as a function of depth for different values

of accelerating energy E_0 in $\text{Al}_{0.5}\text{Ga}_{0.5}\text{N}$. The local temperature rise increases with decreasing of E_0 , because the generation volume depends on E_0 . In case of small values of E_0 , the total of phonons generated by the electron beam is located in a small volume, so the temperature rise becomes important [10]. Consequently, the researchers should take into account this increasing of temperature in nano-characterization by electron beam techniques, because in this case we use small values of E_0 .

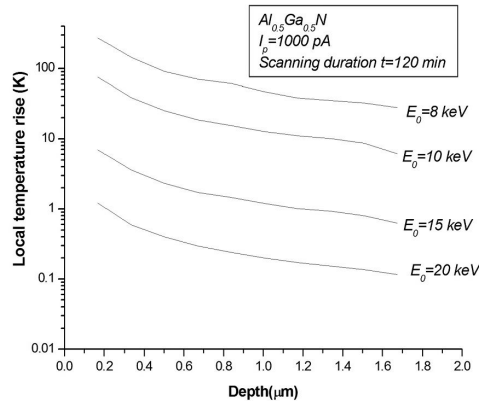


Fig. 4. Local temperature rise as a function of depth for different values of accelerating energy E_0 in $\text{Al}_{0.5}\text{Ga}_{0.5}\text{N}$.

3.4. Influence of the probe current

Fig. 5 shows the local temperature rise as a function of depth for different values of probe current I_p (from 100 pA to 1000 pA). The calculation is presented for 120 min as such scanning duration is usually used in the laboratories. At the surface, a very high temperature rise ($\Delta T > 100$ K) can be achieved with a very intense beam I_p (about 1000 pA) for a few keV of electron energy ($E_0 = 8$ keV). The increase in temperature rise is very sensitive to the primary current I_p . On the other hand, the temperature rise takes very high values at the surface layers (20 nm and 250 nm), then significantly decreases to a very low value in the deeper layers. Therefore, the effect of heating decreases with depth and becomes negligible in the deeper layers (up to 300 nm). This dramatic decreasing of the temperature rise may be due to

the fast phonons generation (phonons excess), and alternatively, due to the weak thermal conductivity of material.

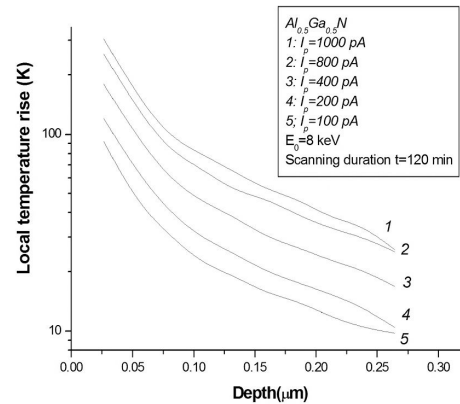


Fig. 5. Local temperature rise as a function of depth for different values of probe current I_p in $\text{Al}_{0.5}\text{Ga}_{0.5}\text{N}$.

3.5. Influence of scanning duration

One of parameters influencing SEM analysis is the scanning durations. To calculate the influence of analysis duration, we used the Monte Carlo-dynamic molecular method (hybrid model) [11]. Fig. 6 shows the local temperature rise as a function of depth for different values of scanning duration t (radiation duration). To avoid the electron beam heating, it is preferable to use short durations in the scanning experiments.

Remark: The calculation step in depth is not the same in Fig. 3, Fig. 4, Fig. 5 and Fig. 6, so this change in the calculation step can have a slight influence on the calculation accuracy.

4. Conclusion

According to obtained results, the electron beam can modify (under testing) the results of material characterization at low dimensions due to electron beam heating, which depends on electron beam parameters (accelerating voltage, primary current and scanning duration). A hybrid numerical model (Monte Carlo-dynamic molecular)

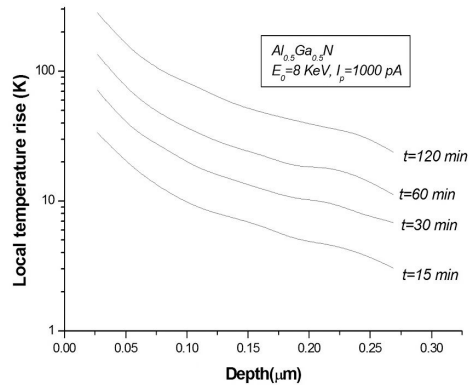


Fig. 6. Local temperature rise as a function of depth for different values of scanning duration t (radiation duration) in $\text{Al}_{0.5}\text{Ga}_{0.5}\text{N}$.

has been employed to investigate the local temperature rise during the electron beam characterization of $\text{Al}_x\text{Ga}_{1-x}\text{N}$. These results must be taken into account in the electron beam scanning techniques, in particular at low dimensions. For example, the cathodoluminescence (CL) spectra are obtained for the real temperature (room temperature + local temperature rise) not for the room temperature only, so the CL spectra must be shifted (corrected) in order to obtain the real optical and electrical properties.

References

- [1] MORKOÇ H., STRITE S., GAO G.B., LIN M.E., SVERDLOV B., BURNS M., *J. Appl. Phys.*, 76 (1994), 1363.
- [2] GOLDBERGER J., HE R., ZHANG Y., LEE S., YAN H., CHOI H.J., YANG P., *Nature*, 422 (2003), 599.
- [3] BARJON J., BRAULT J., DAUDIN B., JALABERT D., SIEBER B., *J. Appl. Phys.*, 94 (2003), 2755.
- [4] GELHAUSEN O., PHILLIPS M.R., TOTTH M., *J. Appl. Phys.*, 89 (2001), 3535.
- [5] FLEISCHER K., TOTTH M., PHILLIPS M.R., ZOU J., LI G., CHUA S.J., *Appl. Phys. Lett.*, 74 (1999), 1114.
- [6] YACOBI B.G., HOLT D.B., *Cathodoluminescence Microscopy of Inorganic Solids*, Plenum Press, New York, 1990.
- [7] TALMON Y., THOMAS E.L., *J. Microsc.-Oxford*, 111 (1977), 151.
- [8] TALMON Y., THOMAS E.L., *J. Microsc.-Oxford*, 113 (1978), 69.
- [9] RANDOLPH S., FOWLKES J., RACK P., *J. Appl. Phys.*, 97 (2005), 124312.
- [10] NOURI A., CHAGUETMI S., BELABED N., *Surf. Interface Anal.*, 38 (2006), 1153.
- [11] NOURI A., *Res. J. Mater. Sci.*, 2(2014), 1.
- [12] NOURI A., LEGHRIB L., AOUATI R., *Glob. J. Adv. Pure Appl. Sci.*, 6 (2015), 08.
- [13] PARK Y.S., PARK C.M., LEE S.J., KANG T.W., *J. Appl. Phys.*, 97 (2005), 073516.
- [14] REUTER P., RATH T., FISCHEREDER A., TRIMMEL G., HADLEY P., *Scanning*, 33 (2011), 1.
- [15] LETHY K.J., EDWARDS P.R., LIU C., SHIELDS P.A., ALLSOPP D.W.E., MARTIN R.W., *Semicond. Sci. Tech.*, 27 (2012), 085010.
- [16] BARIN I., KNACKE O., KUBASCHEWSKI O., *Thermochemical Properties of Inorganic Substances*, Springer-Verlag, Berlin, 1977.
- [17] WEILI L., ALEXANDER A.B., *Appl. Phys. Lett.*, 85 (2004), 5230.
- [18] KANAYA K., OKAYMA S., *J. Phys. D Appl. Phys.*, 5 (1972), 43.
- [19] EVERHART T., HOFF P., *J. Appl. Phys.*, 42 (1971), 5837.
- [20] WITTRY D.B., KYSER D.F., *J. Appl. Phys.*, 38 (1967), 375.
- [21] AS D.J., POTTHAST S., KÖHLER U., KHARTCHENKO A., LISCHKA K., *Mater. Res. Soc. Symp. Proc.*, 743 (2003), L5.4.1.

Received 2017-02-28

Accepted 2018-03-18